Nanoscale

ROYAL SOCIETY OF CHEMISTRY

MINIREVIEW

View Article Online
View Journal | View Issue

Cite this: *Nanoscale*, 2021, **13**, 19828

Artificial interphase engineering to stabilize aqueous zinc metal anodes

Zichao Yan, Wenli Xin and Zhiqiang Zhu *

Aqueous Zn-ion system combining the advantages of energy density, intrinsic safety, and environmental benignity, has been regarded as a promising power source for future electronics. Besides cathodes and electrolytes, more attention should be paid to stabilizing zinc metal anodes since the main challenges in current aqueous Zn-ion batteries are still the hydrogen evolution and dendrite growth of the zinc anode. Thereupon, artificial interphase engineering that integrates the highly tunable, selectable, and controllable characteristics becomes one of the most effective ways to stabilize zinc anodes. In this mini-review, state-of-the-art knowledge on the rational interphase engineering of aqueous zinc metal anodes in the functional layer coating and *in situ* solid electrolyte interphase formation are covered. The main focus of this work is to summarize the most recent development of artificial interphases in chemical composition, structure, and function. The potential issues and perspectives regarding materials and methods are presented.

Received 14th September 2021,
Accepted 10th November 2021

DOI: 10.1039/d1nr06058a

rsc.li/nanoscale

1. Introduction

The development of energy storage devices with high energy density and addressing safety issues is a constant topic that people have pursued all the time.[1–4] In recent years, battery fires resulting from flammable organic electrolytes and highly active alkalis metal anodes (Li and Na) have further stimulated the research interests in safer batteries.[5–8,63,64] To meet the goal, batteries that are assembled in aqueous electrolytes and can be utilized for a long period of time without safety and reliability issues, will be of broad interest to society.[9] Aqueous Zn-ion batteries (AZIBs) that consist of nonflammable electrolyte (water) and stable anode (metallic zinc) are promising for large-scale energy storage owing to their intrinsic safety, low cost, and environmental benignity. Undoubtedly, the utilization of metallic zinc (Zn) with high specific capacity (820 mA h g^{-1}) and low redox potential (−0.76 V *vs.* the standard hydrogen electrode) can realize a competitive energy density.

State Key Laboratory of Chemo/Biosensing and Chemometrics, College of Chemistry and Chemical Engineering, Hunan University, Changsha 410082, China.
E-mail: zqzhu@hnu.edu.cn

Zichao Yan

Zichao Yan received his PhD degree in the Institute for Superconducting and Electronic Materials, University of Wollongong, Australia in 2020. He is currently an Assistant Professor at Hunan University, China. His research has been focused on energy storage materials for battery applications, especially on novel composite materials and new electrolytes for sodium/zinc-based storage systems.

Zhiqiang Zhu

Zhiqiang Zhu is a Full Professor at the College of Chemistry and Chemical Engineering at Hunan University, China. He received his B.S. (2010) and Ph.D. (2015) from Nankai University under the supervision of Prof. Jun Chen. After working as a research fellow at Prof. Xiaodong Chen's group at Nanyang Technological University, he started his independent research career as a Full Professor at Hunan University in December 2019. His current research interests focus on functional materials for rechargeable batteries.

However, the main challenges in current AZIBs are still the hydrogen evolution and dendrite growth of the zinc anode, which could result in low Coulombic efficiency (CE) and a short lifespan.[10] To address the above concerns, the following suggestions have been proposed: (i) the zinc anode should have a stable electrode/electrolyte interphase, which represents their abilities for prolonging the cycle life and the practical requirements of rechargeable batteries.[11] (ii) The irreversible by-products on the Zn surface, such as ZnO and $Zn_4(OH)_6SO_4{\cdot}xH_2O$ should be minimized, which would promote zinc dendrite growth and corrosion.[1] More specifically, the generated inactive by-products, passivating the zinc anode surface, would further block the transport of Zn^{2+}. (iii) The electrolyte compatibility of the Zn anode should be considered. The huge charge transfer resistance during the plating and stripping processes of Zn^{2+} would cause energy consumption and poor rate performance.[12] Experimentally, regulating the interface between the electrolyte and Zn anode by functional electrolyte additives or solid electrolyte interphase engineering may aid in reducing resistance.[13] (iv) The failure of batteries in different application scenarios is different from one to another.[14–16] For instance, water molecules that evaporate under high temperatures may accelerate the dehydration process, leading to the deterioration of electrochemical performance. At subzero temperatures, water would freeze and inhibit the ion transportation of an aqueous electrolyte.[17] Therefore, all components inside, or outside the battery, including working conditions (temperature, current, voltage) and cathode systems (the additives may have side effects on the cathode) should be considered before discussing their performance.

The strategy of artificial interphase engineering integrates the highly tunable, selectable, and controllable characteristics, which becomes one of the simplest and most effective ways to improve the stability of Zn anodes.[18,19] Compared to other strategies such as electrolyte regulating and host materials design, artificial interphase engineering aims to directly tailor the anode/electrolyte interphase to suppress severe interfacial reactions, showing great potential towards practical applications.[11,20] Thus, a comprehensive summary and outlook of recent progress for interphase engineering of Zn anode are of great importance for the development of AZIBs. Although the introduction of the artificial interphase engineering of zinc anode has been briefly discussed elsewhere,[9–11] a detailed discussion on the classification, functions, and design principles of the artificial interphases is lacking. This mini-review presents a comprehensive summary of the state-of-the-art knowledge on the rational interphase design to stabilize aqueous zinc metal anodes. The chemical composition, structure, functions, design principles, and methods of artificial interphases will be discussed in detail (Fig. 1).

2. Functions of artificial interphases

Despite the high safety and low cost of AZIBs, the undesired side reactions associated with hydrogen evolution reaction

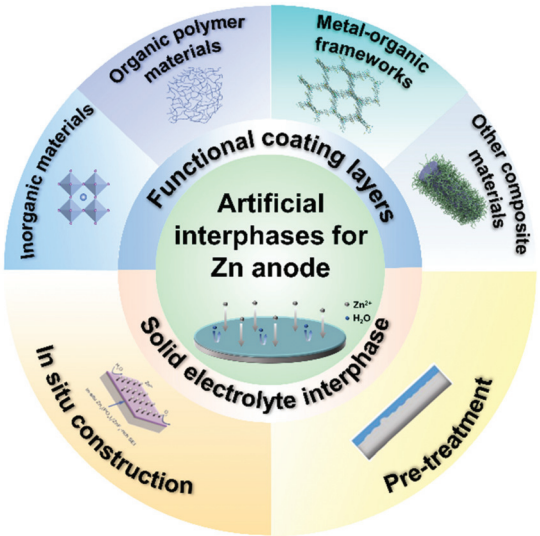

Fig. 1 Schematic of strategies for artificial interphases such as functional coating layers and solid electrolyte interphases by means of materials design and interface engineering.

(HER), dendrite growth, surface corrosion, and by-products formation, are still occurring at the Zn surface.[21] Even worse, those complicated side reactions would further accelerate each other, leading to low CE and poor cycle life. For example, HER (eqn (1)) inevitably occurs during the zinc plating process, since the standard electrode potential of H^+/H_2 (0 V *vs.* SHE) is higher than that of Zn^{2+}/Zn.[22]

$$2H_2O + 2e^- \rightarrow 2OH^- + H_2 \uparrow \quad (1)$$

The previous research has proved that the local content of OH^- ions near the anode surface increases as the HER progresses, which would accelerate the formation of the passivating layer (such as Zn hydroxides) on the Zn surface.[23] Upon the by-products accumulating, the insulative passivate layer can act as a barrier to prevent the deposition and dissolution of zinc anodes, resulting in the consumption of active Zn^{2+} and the formation of "dead" Zn.[24] Thermodynamically, nucleation of Zn^{2+} ions favours the sites with a lower energy barrier, while, the uneven surface corrosion by the above-mentioned side reactions would further trigger the "tip effect", causing wild growth of zinc dendrites.[25]

Apparently, the side reactions are closely relevant and generally occur at the Zn/electrolyte interphase, therefore, artificially regulating the interphases would be of great help in improving the performance of AZIBs. Firstly, the construction of artificial interphase with high Zn affinity could solve the problem of Zn^{2+} ions deposition.[26] While, its value should not be too high or too low. If the Zn affinity is too high, the plated Zn dendrites tend to grow vertically, causing the battery failure. It cannot be too low as well, which is a key criterion to judge its applicability. Actually, the value of Zn affinity is a comparative value in different reference systems and situations, the conductivity of the designed interfacial layers

should be discussed, especially for high Zn affinity layers. Secondly, the hydrophily of the interfacial layer is a key factor for the interfacial impedance, polarization, and reaction kinetics.[27] The unwelcome water molecules can be blocked by the hydrophobic interfacial layer, while the increased interfacial impedance and polarization would cause sluggish kinetics. Thus, the thickness and ion-conductivity of the interfacial layer should be considered for the hydrophobic interfacial layer. Similarly, proper hydrophilicity of artificial interphase can easily access electrolyte ions to the anode surface, thus improving reaction kinetics, while the side reaction resulting from water molecules would cause the battery failure. Therefore, the porous or dense characteristics of the interfacial layer should be discussed in the hydrophilic interfacial layer. Anyway, artificial interphase as the electrochemically and mechanically stable interface layer could effectively isolate both H_2O molecules and electrolyte anions to suppress corrosion reaction, promoting Zn^{2+} transport and reaction kinetics.[28] Thus, designing artificial interphases with favourable functions, including adjusting interfacial electric field, isolating bulk electrolyte, conducting zinc ions, and regulating crystal orientation, has been regarded as one of the best strategies to improve the stability of zinc anodes.

3. Artificial interphases for Zn anode

In the past decade, research efforts in Zn batteries are mainly focused on the development of high-performance cathode materials which undoubtedly helped to optimize the electrochemical performance, but it is not the only determinant of performance in practical applications.[29,61,62] The Zn anode serving as the source of Zn^{2+} also plays a non-negligible role in AZIBs. Looking back to the history of lithium–sulfur batteries, the research interests are generally moved from cathode to anode, since scientists realized that Li dendrites are the major obstacle for practical applications.[30] Similar to lithium–sulfur batteries, although recent advances in cathode materials have improved the electrochemical performance of AZIBs, the unstable anode/electrolyte interphase-caused parasitic reactions will eventually affect its applications in the long run. In view of the consequences, the construction of robust artificial interphase to generate a moderate chemical environment for uniform Zn plating/stripping is essentially needed for practical AZIBs. Generally, functional layers coating and *in situ* SEI formation are the main strategies to build chemically and electrochemically stable, mechanically robust artificial interphases.

3.1 Functional coating layers

In an aqueous electrolyte, the construction of an effective surface coating layer is an efficient way to stabilize the active metal anodes.[11] In the case of AZIBs, the coating layer acts as a buffer interphase to avoid direct contact of Zn metal with the aqueous electrolyte, thus it can make full use of the high specific capacity of metal anodes, and suppress the dendrite growth and parasitic reactions. Coating layers directly coated on the Zn metal surface with the thickness of micrometres may not fit for the pouch cell design due to high resistance and polarization. While the *ex situ* designed interfacial materials have only the protective effect for the anode, thus it can apply to match most of the cathode systems. The functions of coating layers variously depend on their chemical composition and structure. For example, the Zn^{2+} ions conductivity of the coating layer has responded directly to the fast-charging capability of AZIBs.[31] The g-C_3N_4 modulating interface with the uniform nucleating electron field (the rich N species) and fast electron transport (3D porous structure and innately rich structural defects) prompted the formation of strong Zn–N transient states to capture Zn^{2+}, which induce the stabilization and uniformity of Zn distribution to further control the dendrite growth.[32] This mechanism can also be applied to other interfacial layers with strong electronegative atoms, which could offer a lower energy barrier and more homogeneously charged distribution to facilitate highly reversible Zn plating/stripping. Due to the high correlation between the structure and function of coating layers, various materials in different functions, including inorganics, organic polymers, metal–organic frameworks, and other composites, have been utilized in designing stable coating layers for Zn anode.

3.1.1 Inorganic materials. Inorganic materials, benefiting from their high mechanical intensity, good chemical stability, and stable corrosion resistance, are widely studied as coating layers to stabilize aqueous Zn metal anodes. Compared to bare Zn anode, zinc chalcogenides that feature strong electronegativity and intrinsically low electrical conductivity are generally assumed to be tightly bound with Zn^{2+} by the anions of zinc chalcogenides, thus enabling long-term Zn dendrite-free plating/stripping and preventing the Zn anode from side reactions of HER and Zn corrosion.[33] In this respect, Cao *et al.*[31] proved that the zinc phosphorus coated on Zn foil (Zn@ZnP) could stabilize the Zn stripping/plating processes, mainly due to the fast ion transfer and electrochemical activation energy reducing capabilities of phosphorus atoms in the coating layer. In particular, the formed ZnP solid solution alloy further expanded the interplanar spacing of the (002) and (101) facet of Zn anode by entering the P atom to the Zn lattice, resulting in excellent high-rate performance in both the Zn/Zn symmetric cell and Zn/MnO_2 full cell (Fig. 2a–c). Compared to atom entering, Ma *et al.*[34] found that the F atoms of the ZnF_2 layer could form tight electrovalent bonds with Zn atoms, giving the credit the charge migration between Zn and F atoms and charge redistribution. The Zn nucleation sites for the ZnF_2 layer can be attributed to the electronegative F atoms, which could greatly limit electron delocalization, providing Zn nucleation sites with lower nucleation overpotential. With high ionic conductivity and improved H_2O-resistant properties of the ZnF_2 layer (Fig. 2d), the Zn@ZnF_2 anode offered a 2500 h cycling performance in the symmetric cell at a current density of 5 mA cm^{-2} with an areal capacity of 1 mA h cm^{-2} (Fig. 2e). In addition to the dense zinc chalcogenides, coating layers with porous structures are also believed to have a high impact to suppress the electrolyte-induced side reactions. The

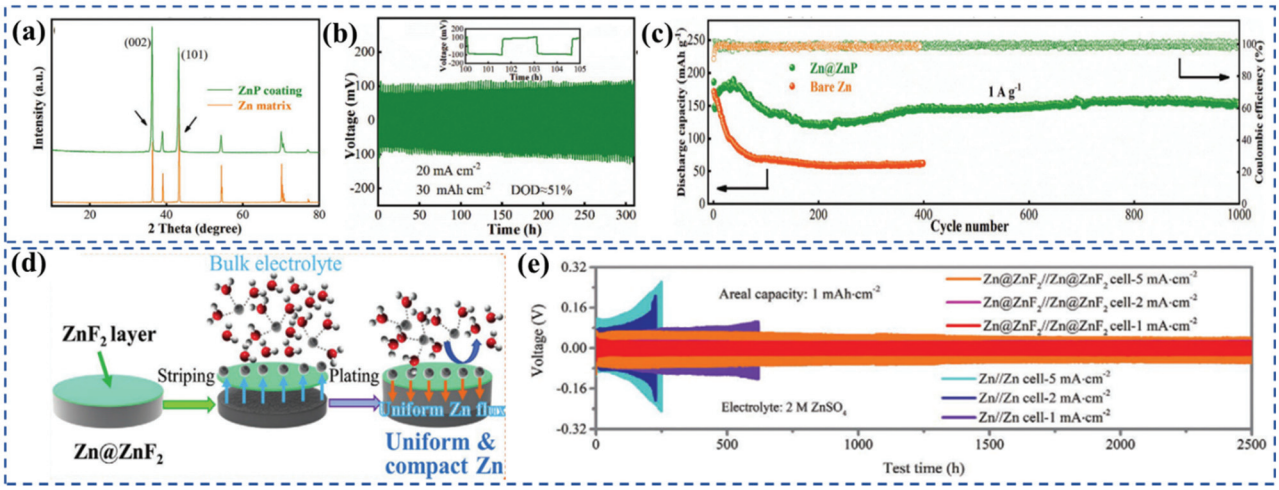

Fig. 2 (a) Grazing incidence XRD (GIXRD) of ZnP coating and Zn matrix. (b) Cycling performance of symmetries cell with Zn@ZnP anode at 20 mA cm^{-2}/30 mA h cm^{-2}. (c) long-term cycling performance at 1 A g^{-1}. Adapted from ref. 31, with permission from Wiley © 2021. (d) Schematic illustration of Zn deposition on Zn@ZnF_2 foil; the ZnF_2 layer endows a dense and dendrite-free Zn deposition by regulating Zn^{2+} diffusion, controlling nucleation, and prohibiting the permeation of H_2O and O_2. (e) Comparison of cycling stability of bare Zn||Zn symmetric cells and Zn@ZnF_2||Zn@ZnF_2 symmetric cells at 1, 2, and 5 mA cm^{-2} with a capacity of 1 mA h cm^{-2}. Adapted from ref. 34, with permission from Wiley © 2021.

artificial interphases consisting of nanoscale materials are of broad interest the researchers since their advantages in building porous protecting layers, uniforming the nucleation sites, constructing highly ordered nanochannels, and adjusting interfacial electric fields, *etc*. Kang *et al.*[35] coated a porous nano-$CaCO_3$ protection layer on the Zn anode surface to improve the stability of the Zn anode during the plating/stripping. Unlike the dense layer function in isolating electrolytes, the porous nano-$CaCO_3$ coating layer aimed to guide uniform electrolyte flux and confined Zn plating reactions at the surface region of the Zn anode, thus suppressing the dendrite growth (Fig. 3a and b). Therefore, the porous nano-$CaCO_3$ coated Zn cell worked well within a test period of 836 h, with only a very gradual and small polarization increment from 80 to 105 mV, which was far better than the 55 h lifespan of bare Zn cell (Fig. 3c). It is well known that the formation of Zn dendrite can be specified into nucleation and growth. The nucleation process is the initial stage of Zn deposition, its uniformity is driven by the electric field, energy barrier, and surface condition. Based on this point, Liang *et al.*[36] prepared a highly reversible Zn anode by coating Zn^{2+} transportable nanoparticles, which could provide uniform nucleation sites through the favourable Maxwell–Wagner polarization of the nanoparticles (Fig. 3d). Benefiting from the high dielectric constant of the ZrO_2 coating layer, the induced Maxwell–Wagner polarization not only decreased the interface impedance but also provided more controllable nucleation sites, leading to uniform Zn plating/stripping and fast reaction kinetics. Consequently, the low polarization (24 mV at 0.25 mA cm^{-2}), high CE (99.36% at 20 mA cm^{-2}), and long cycle life (over 3800 h at 0.25 mA cm^{-2}) were obtained for the ZrO_2-coated Zn anode (Fig. 3e and f).

Lately, the inorganic coating layers with high ionic conductivity and low electrochemical activity are showing great benefits for high-rate and long-life Zn metal anodes. For example, $NaTi_2(PO_4)_3$ (NTP), a typical fast ion conductor, has been demonstrated to improve the internal transport/mobility of Zn^{2+} due to its capability of "ion passable fence", enabling the highly reversible Zn deposition in a Zn/MnO_2 cell even at 10 C (105 mA h g^{-1} with a CE nearly 100% after 10 000 cycles).[37] Zn affinity is an important parameter that affects the electrochemical performance of aqueous batteries. Considering the effects of crystal orientation in adjusting Zn affinity, Zhang *et al.*[38] revealed that the (0 0 1) faceted TiO_2 with −0.63 eV binding energy of Zn^{2+} showed a relatively low Zn affinity than the (1 0 0) facet of TiO_2 (−0.95 eV), which effectively prevented Zn dendrites from growing vertically and thus realized homogeneous zinc deposition. Besides, inorganic materials with layered structures also showed good mobility and transportation toward Zn^{2+}. The layered structure of kaolin with sieve-element function (selective channel of Zn^{2+}) and uniform-pore distribution (≈3.0 nm) has been proposed to modulate the transference of Zn^{2+} while isolating bulk electrolyte from the metal Zn, alleviating the dendritic growth and corrosion.[39] Later, montmorillonite was used to protect the Zn anode, ensuring a high Zn^{2+} transference number ($t_+ \approx 0.82$) and ionic conductivity ($\sigma \approx 3.93$ mS cm^{-1}) during the electrochemical process.[40] Similar to the above-layered structure, Yang *et al.*[41] presented that the Zn-ion diffusion channels for fast Zn^{2+} diffusion and stable Zn^{2+} flux between the electrode/electrolyte interface could also be achieved using an Mg–Al layered double hydroxide (LDH) coating layer.

3.1.2 Organic polymer materials. Apart from designing inorganic coating layers, polymer coating as one of the widespread anti-corrosion technique has been utilized to prohibit the contact of Zn with the corrosive electrolytes.[42,43] Owing to the high viscoelasticity, decent flexibility, and possession of

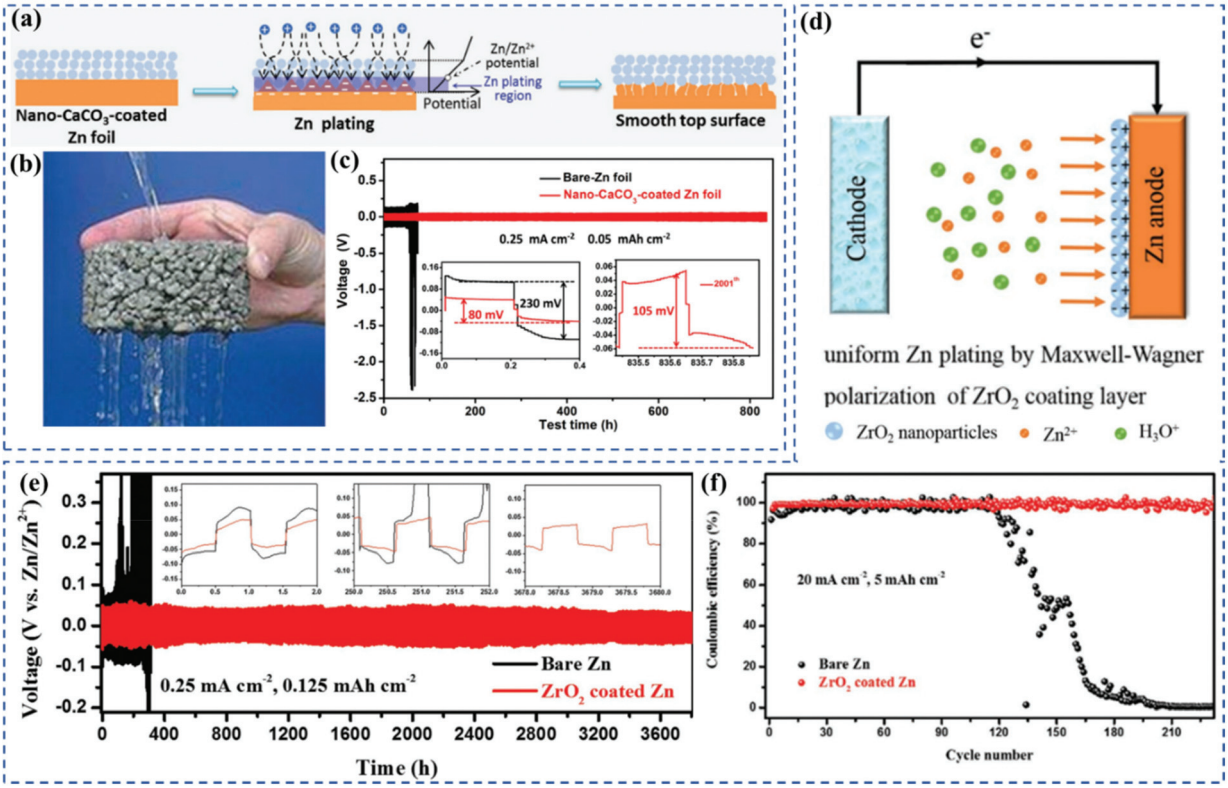

Fig. 3 (a) Schematic illustrations of morphology evolution for bare and nano-$CaCO_3$-coated Zn foils during Zn stripping/plating cycling. (b) The pores in filter papers should act as "highways" for electrolyte transport, similar to the role played by pores in water-permeable bricks. (c) Typical GCD profiles of Zn|$ZnSO_4$ + $MnSO_4$|Zn symmetric cells with bare (black) and nano-$CaCO_3$-coated (red) Zn electrodes at a current density of 0.25 mA cm^{-2}. The amount of Zn deposited in each cycle is 0.05 mA h cm^{-2}. Insets, the first (left inset) and the last (2001th, right inset) detailed voltage profiles of cells with bare (black) and nano-$CaCO_3$-coated (red) Zn electrodes. Adapted from ref. 35, with permission from Wiley © 2018. (d) In these cells, filter papers were employed as separators. Schematic the stripping/plating processes of the ZrO_2-coated Zn anode. (e) Voltage profiles of the metallic Zn plating/stripping in Zn symmetric full-cell and ZrO_2-coated Zn symmetric full-cell at 0.25 mA cm^{-2} for 0.125 mA h cm^{-2}. (f) CE of Zn plating/stripping in the Zn||Ti half-cell and the ZrO_2-coated Zn||Ti half-cell at 20 mA cm^{-2} with 5 mA h cm^{-2}. Adapted from ref. 36, with permission from Wiley © 2020.

intrinsic amide groups, polyamide was chosen as the coating layer to elevate the nucleation barrier and restrict the 2D diffusion of Zn^{2+}.[20] It has been proved that the finer size and high density of nucleus seeds of the polyamide coating layer effectively regulated the aqueous Zn deposition behavior, thus providing a 60-fold enhancement in the cycle life (over 8000 hours) compared to the polyamide-free anode. To further understand the mechanism of zinc plating/stripping in the polyimide coating layer, Zhu *et al.*[44] prepared a polyimide-coated Zn anode that resolved the above doubts. The reason behind this was confirmed from the electrostatic potential calculation and X-ray photoelectron spectroscopy of the polyimide (Fig. 4a–d). The negative parts concentrating on the carbonyl oxygen atoms of polyimide acted as electron-donating sites were available for coordinating with Zn ions in the electrolyte, which could minimize the concentration gradient, offering fast reaction kinetics and low overpotential for Zn^{2+} plating and stripping (Fig. 4e and f). Considering the water-repellent capability of polymers, another new class of coating layers, the ionic liquid (IL) skinny gels, were reported to stabilize the anode/electrolyte interphase (Fig. 4g).[22] Boosted by the IL solvent, Zn salts, and thiol–ene polymer compliant skeleton, the Zn/Zn symmetric cell presented a stable and sustainable cycling performance over 1000 h, as well as the Zn/MnO_2 full cell (capacity retention ≈95.7% after 600 cycles) (Fig. 4h and i), indicating that the coating layer not only avoided the access of water molecules but also enabled fast and stable Zn^{2+} conduction.

3.1.3 Metal–organic frameworks. The most recently reported metal–organic frameworks (MOFs) with spatial confinement effects are introduced as functional layers to effectively modulate the diffusion, nucleation, and deposition of Zn^{2+}.[9,45] The highly ordered nanochannels and N species of the zeolitic imidazolate framework-8 (ZIF-8) have been proven to be effective protection layers in homogenizing Zn^{2+} flux distribution and modulating the plating/stripping rate.[46] Consequently, the ZIFs coated Zn anode showed a 1200 h lifespan with a low polarization at 2 mA cm^{-2} in the symmetric cell, and outstanding cycling performance of 10 000 cycles in the $LaVO_4$//Zn@ZIF full cell (Fig. 5a and b). To form an inti-

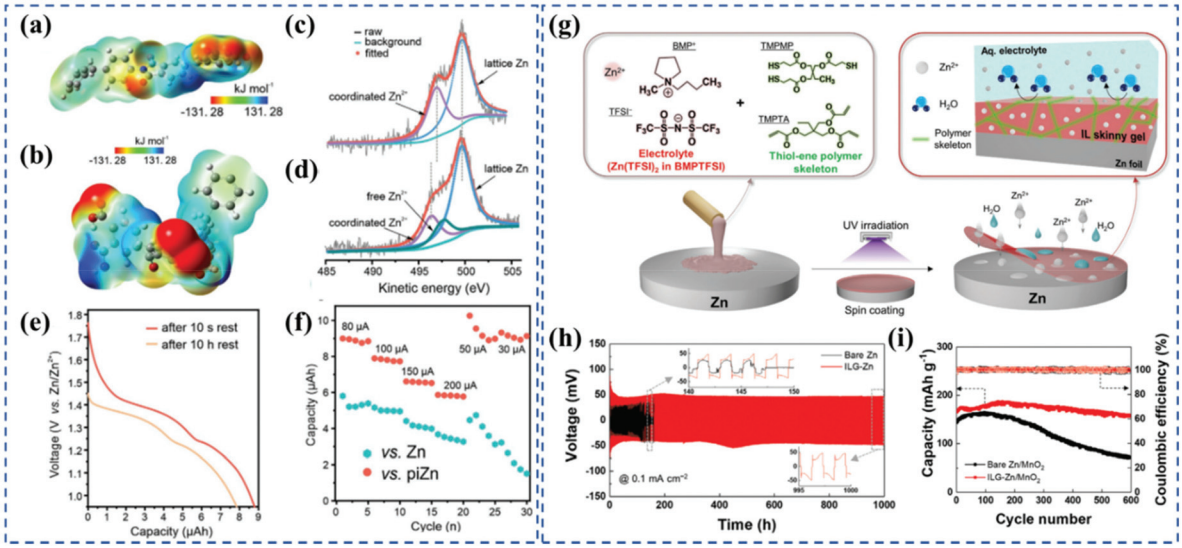

Fig. 4 (a) ESP of the polyimide. (b) ESP of the cycled polyimide. (c) Zn LMM Auger spectrum of piZn before cycling. (d) Zn LMM Auger spectrum of piZn after cycling. (e) Discharge curves of a fresh piZn microbattery and that after the rest of 10 h at the fully charged state. (f) Comparisons of rate performance of the Zn and piZn microbattery. Adapted from ref. 44, with permission from Wiley © 2021. (g) Schematic illustration depicting the fabrication of an IL skinny gel on a Zn anode, along with its chemical structure and role as a water-repellent ion-conducting protective layer. (h) Galvanostatic Zn plating/stripping cyclability of the AE-containing Zn/Zn symmetric cells (ILG-Zn *vs.* bare Zn) at an areal capacity of 0.1 mA h cm^{-2} and a current density of 0.1 mA cm^{-2}. (i) Charge/discharge cycling performance (bare Zn *vs.* ILG-Zn) at a current density of 2 C. Adapted from ref. 22, with permission from Wiley © 2021.

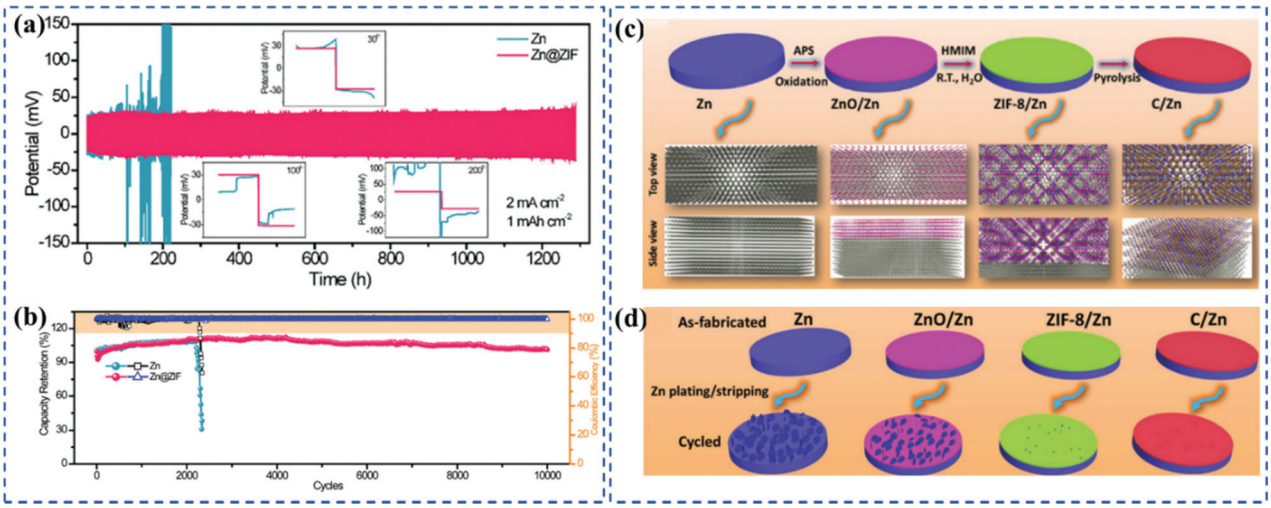

Fig. 5 (a) Voltage profiles of symmetric cells based on bare Zn foil and Zn@ZIF anodes at 2 mA cm^{-2} with a capacity of 1 mA h cm^{-2}. (b) Cycling performance and CE tested at 10 mA cm^{-2} for 10 000 cycles of the $LaVO_4$||Zn and $LaVO_4$||Zn@ZIF batteries. Adapted from ref. 46, with permission from Wiley © 2020. (c) Schematic of the Zn anode fabrication process and the predicted top and side views of the structures. (d) Schematic of dendritic Zn flake formation on Zn anodes during Zn plating–stripping. Adapted from ref. 47, with permission from Wiley © 2020.

mate ZIF-8 layer, Yuksel *et al.*[47] built an etchable ZnO layer on the Zn surface, by etching, which then produced Zn^{2+} ions that were able to coordinate with the 2-methylimidazole, *in situ* forming the ZIF-8 layer. Additionally, they revealed that pyrolyzation of the coating layer under a gas flow of H_2/Ar could achieve a hydrophilic and porous surface (Fig. 5c and d). Actually, the contact angle measurement revealed that the coating layer is not 100% hydrophilic, which is a comparative value between different decorates, thus facilitating Zn^{2+} ion diffusion and the production of a uniform charge distribution. This is consistent with Wang's work that the porous structure, trace amount of zinc in the framework, and high over-potential for hydrogen evolution of the annealed ZIF-8 were the reasons behind the dendrite-free Zn plating and stripping.[48]

3.1.4 Other composite materials. The design of composite layers that integrate the merits of various materials has been

recognized as a highly efficient way to suppress dendrite growth. So, Zhao *et al.*[49] constructed a composited matrix, integrating the virtues of TiO_2 nanoparticles and polyvinylidene fluoride, which could not only effectively assist in uniform Zn electrodeposition but also block H_2O/O_2 corrosion, resulting in improved electrodeposition consistency and thermodynamic stability of the Zn anode. Additionally, Cui *et al.*[50] combined the benefits of organic and inorganic structures to design a hybrid protection layer by integrating Zn–X zeolite nanoparticles with Nafion, which shifted ion transport from channel transport in Nafion to a hopping mechanism in the composited interface. With the development of functional materials in the anode coating, more and more new functions and mechanisms by complexing organic–inorganic, organic-organic, or inorganic-inorganic materials will be revealed and broaden the interest of the researchers.[51–53]

In addition to the functions of coating layers in suppressing dendrites and side reactions, the high polarization value caused by the coating strategy, which is a common type of battery failure, should also be taken into account. For example, the resistance of the polyimide coating layer is estimated to be 1500 Ω, much higher than the transfer resistance at the Zn/electrolyte interface,[44] which could probably result in low CE of Zn plating/stripping and low Zn utilization in long-term cycling. Considering the increased internal impedance/polarization arising from the barrier effect of the protective layers, future research works focused on the coating layers with nano-thick features and high ionic conductivity are highly emphasized to reduce the overpotential of the Zn plating/stripping, kinetically. Besides, the physical coating is hard to form even interphase for Zn deposition, thereby chemically bonding the coating layer and Zn metal at the atomic level are strongly recommended in future work, which would fundamentally lower the energy barrier of Zn^{2+} transferring between the protective layer and Zn anode.

3.2 Solid electrolyte interphase

Since the dense Zn^{2+} conductive SEI film is absent in AZIBs, the unstable anode/electrolyte interphase usually causes a series of undesired interfacial reactions.[54] Inspired by the batteries operated under organic electrolytes, artificially forming a stable SEI film would dramatically aid the development of high-rate and long-life AZIBs.

The properties of SEI films are highly associated with the synthesis methods, which are generally classified into surface pre-treatment and *in situ* construction types. For surface pre-treatment, Hao *et al.*[55] built an artificial ZnS interphase on the Zn surface by a vapor–solid strategy to enhance the reversibility of Zn plating/stripping (Fig. 6a). The charge distribution on ZnS not only enhanced the Zn^{2+} diffusion at the ZnS@Zn interphase but also increased the adhesion of the ZnS film to the Zn surface, providing a smaller voltage polarization and longer lifespan of the symmetrical cell for >1100 h at 2 mA h cm^{-2} compared to the bare Zn cells (Fig. 6b). The vapor–solid strategy could easily adjust the thickness and homogeneity of the SEI film, offering an in-depth study of Zn metal surface chemistry. Similarly, ZnSe film was also fabricated by exposing Zn foil in a vapored Se atmosphere (Fig. 6c).[56] It has been

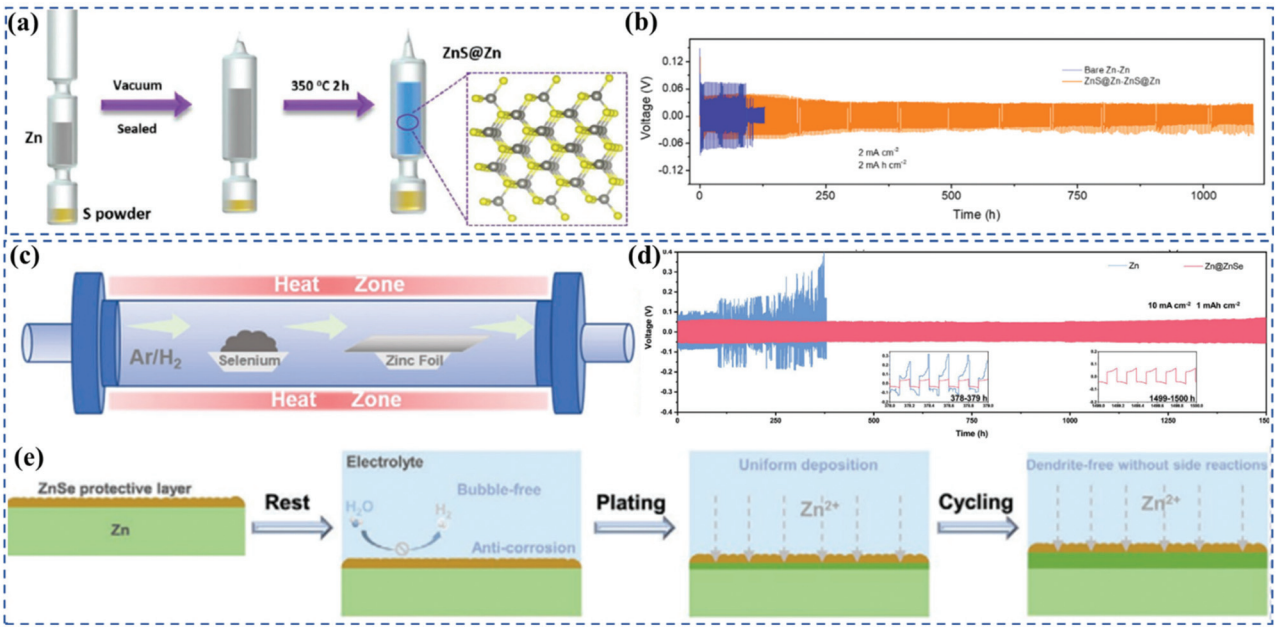

Fig. 6 (a) Introducing the ZnS layer on the surface of Zn metal substrate by an *in situ* strategy. (b) Comparison of the cycling stability of bare Zn symmetric cell and ZnS@Zn-350 symmetric cell at 2 mA cm^{-2} with the capacity of 2 mA h cm^{-2}. Adapted from ref. 55, with permission from Wiley © 2020. (c) Illustration of synthesis of Zn@ZnSe. (d) Long-term cycling test at a high rate of 10 mA cm^{-2} with 1 mA h cm^{-2} for the bare Zn and Zn@ZnSe cells. (e) Schematic illustration of the side reactions and Zn plating behaviours of the Zn@ZnSe in their whole lifecycle. Adapted from ref. 56, with permission from Wiley © 2021.

reported that the anticorrosion and HER suppressing capabilities of the ZnSe film provided a notable rate of performance and cycling stability (1500 h) even at 10 mA cm^{-2} with 5 mA h cm^{-2} (Fig. 6d and e). In addition to the vapor–solid strategy, Xu *et al.*[57] simply immersed a Zn plate into $CuSO_4$ solution for a short period of time to form a uniform and robust SEI layer ($Zn_4SO_4(OH)_6{\cdot}5H_2O/Cu_2O$), which homogenized the electric field distribution and controlled the dendrite growth, leading to a long lifespan of more than 1400 h and a high average CE of 99.2% at 2.0 mA cm^{-2} and 2.0 mA h cm^{-2}.

Even the pre-treated SEI films maintained a stable cycling performance, the lack of self-repairability is still a problem in the long run.[24] Therefore, the strategy of *in situ* construction, adding functional additives to assist the *in situ* formation of stable SEI films, is a good choice for uniform Zn plating and dense zincophobic SEI growth. Cao *et al.*[24] *in situ* synthesized a zincophilic–zincophobic ($Sn/Zn_5(OH)_8Cl_2{\cdot}H_2O$) SEI film by using a eutectic 7.6 m $ZnCl_2$ aqueous electrolyte with 0.05 m $SnCl_2$ additive. It is worth noting that the *in situ* produced zincophilic Sn could tightly anchor Zn foil, and further facilitate the formation of a zincophobic $Zn_5(OH)_8Cl_2{\cdot}H_2O$ film, suppressing Zn dendrite growth and water decomposition (Fig. 7a and b). With the special design, the Zn/$VOPO_4$ full cells showed >95% capacity with a CE of >99.9% for 200 cycles at −50 °C, and retained 30% capacity at −70 °C of that at 20 °C (Fig. 7c–e). Besides, Li *et al.*[25] found that the above robust SEI films could also be achieved at a low-concentration bi-salt Zn $(OTF)_2$–$Zn(NO_3)_2$ electrolyte. They revealed that the self-terminated chemical reaction of NO_3^- with Zn^{2+} and OH^- generated *via* HER could guide the formation of a conducting $Zn_5(CO_3)_2(OH)_6$ layer, which in turn promoted the generation of ZnF_2 layer, thus forming the bi-layer SEI film (Fig. 7f). Besides inorganic additives, Cao *et al.*[23] revealed that the decomposition of dimethyl sulfoxide (DMSO) in $ZnCl_2$–H_2O electrolyte could form $Zn_{12}(SO_4)_3Cl_3(OH)_{15}{\cdot}5H_2O$, $ZnSO_3$, and ZnS enriched SEI, which could prevent Zn dendrite and further restrain water decomposition. Later, the alkylammonium salt has also been developed to assist the formation of a robust, Zn^{2+}-conducting, and waterproof SEI.[2] The alkylammonium salt engendered the *in situ* formation of fluorinated and hydrophobic interphase that effectively inhibited the hydrogen evolution reaction. Specifically, this type of SEI not only showed a homogeneous thin film of 64 nm but also enabled strong compatibility with both Zn^{2+}-conducting and waterproof components. However, the hydrophobic interphase formed in an aqueous electrolyte would increase the energy barrier for Zn nucleation/dissolution, thus increasing interfacial impedance and polarization.

Indeed, the *in situ* synthesis of SEI films during the plating and stripping processes of Zn^{2+} would undoubtedly improve its self-repairability, this does not mean that interphase issues, such as hydrogen evolution reaction, dendrite growth, surface corrosion, and by-products formation, have been effectively addressed. Electrolyte additives are normally involved in *in situ* synthesis of the thin SEI films. The thin films with self-repairability have great potential for high-rate cell design due to good kinetics and reasonable resistance. While the synthesis mechanism for SEI films during the electrochemical process is sophisticated, the performance is closely related to the compatibility of all components inside, or outside the battery, including working conditions (temperature, current, voltage) and cathode systems (the additives may have side effects on the cathode). The choice of cathode systems available for the battery with *in situ* synthesized SEI films is limited. As we can

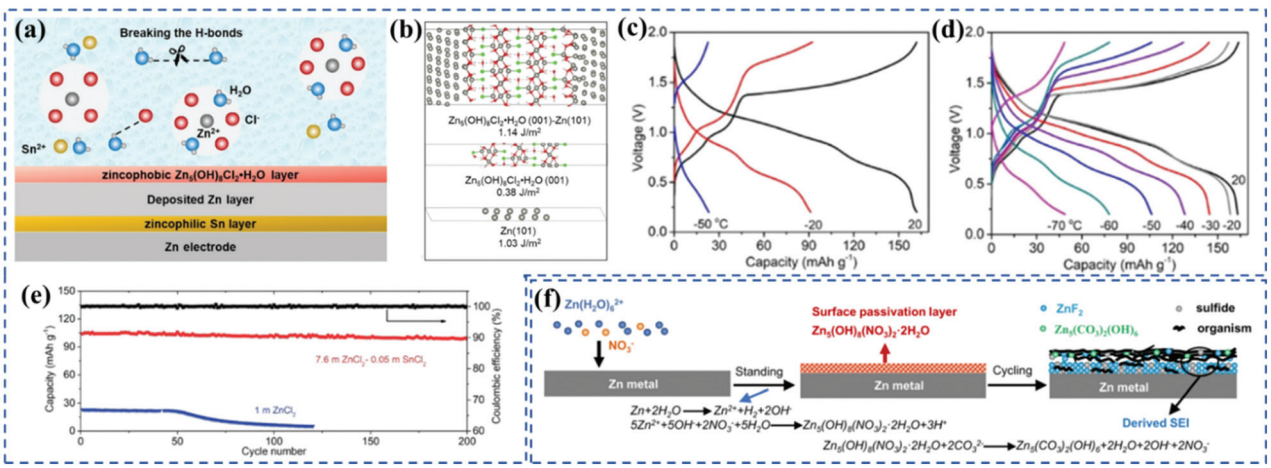

Fig. 7 (a) Scheme of the electrolyte and electrolyte-electrode-interphase structure. (b) Atomic structures and related surface/interfacial energies of $Zn_5(OH)_8Cl_2{\cdot}H_2O$ surface, Zn surface, $Zn_5(OH)_8Cl_2{\cdot}H_2O(001)|Zn(101)$ interface. Electrochemical performance of $VOPO_4$||Zn cells using different electrolytes at different temperatures. Charge/Discharge profiles of VOPO4||Zn cells using. (c) 1 m and (d) 7.6 m $ZnCl_2$–0.05 m $SnCl_2$ electrolytes. (e) Cycling performance of $VOPO_4$||Zn cells using different electrolytes at −50 °C with a charge/discharge current density of 1/3C. Adapted from ref. 20 with permission from the Royal Society of Chemistry © 2019. (f) ZnF_2-$Zn_5(CO_3)_2(OH)_6$-organic SEI formation mechanism. The presence of NO_3^- promotes the formation of electrically and ionically insulating $Zn_5(OH)_8(NO_3)_2{\cdot}2H_2O$ layer (red), which subsequently transforms into an electrically insulating but ionically conductive SEI with ZnF_2-$Zn_5(CO_3)_2(OH)_6$ inner part coated by the organic outer part. Adapted from ref. 21 with permission from the Royal Society of Chemistry © 2020.

Table 1 Summary of properties and electrochemical performance of artificial interphases for AZIBs

Interfacial materials	Types	Characteristics	Major functions	Current density (mA cm^{-2}), capacity (mA h cm^{-2})	Life span (h)	Ref.
In	Functional coating layer	Corrosion inhibitor; nucleating agent	Suppressing Zn corrosion and dendrite growth	0.2, 0.2 1, 1	1500 >500	12
Sn	Functional coating layer	Interconnected 3D nano-channel	Suppressing dendrite growth	1, 1	800	16
Ag	Functional coating layer	Nucleation agent	Guiding uniform Zn nucleation	0.2, 0.2 2, 2	>1400 150	18
CNG	Functional coating layer	Strong tensile force; negative surface charges	suppressing Zn corrosion	0.25, 0.5 1, 0.5	5500 2956	28
g-C_3N_4	Functional coating layer	Zincophilic interphase	Reducing Zn^{2+} diffusion energy barrier; homogeneous charge distribution	2, 2 10, 5	500 120	32
ZnF_2	Functional coating layer	Electronical insulation; Zn^{2+} ion conductive	Suppressing side reactions; harmonizing Zn^{2+} migration	1, 1 10, 10	2500 590	35
ZrO_2	Functional coating layer	High dielectric constant	Enhancing Zn^{2+} transport kinetics; guiding uniform nucleation	0.25, 0.125 5, 1	>3800 >2100	36
F-TiO_2	Functional coating layer	Zincophilic	Suppressing dendrite growth; harmonizing Zn^{2+} migration	1, 1 2, 2	460 280	38
$CaCO_3$	Functional coating layer	Porous structure	Harmonizing Zn^{2+} migration; reducing Zn^{2+} plating rate	0.25, 0.05	>800	35
MMT-Zn	Functional coating layer	Zn^{2+} ion conductive	Suppressing Zn corrosion, passivation, and dendrites growth	1, 0.25 10, 45	>1000 >1000	26
BTO	Functional coating layer	Ion-pumping effect	Enhancing Zn^{2+} transport kinetics	1, 1 10, 5	4100 720	40
HsGDY	Functional coating layer	Zn-ion diffusion channels; robust chemical stability	Harmonizing Zn^{2+} migration	0.5 0.5 2, 2	2400 2400	42
PA	Functional coating layer	Unique hydrogen-bonding network; strong coordination ability	Harmonizing Zn^{2+} migration; suppressing Zn corrosion	0.5, 0.25 10, 10	8000 70	20
COP-CMC	Functional coating layer	Hydrophilic layer	Enhancing Zn^{2+} transport kinetics; guiding uniform nucleation; suppressing Zn corrosion and hydrogen evolution reaction	0.25, 0.05 5, 3	>4000 >2000	43
Polyimide	Functional coating layer	Strong polar oxygen atoms	Enhancing Zn^{2+} transport kinetics; reducing nucleation overpotential	4, 2	300	44
ZIF-8	Functional coating layer	Well-ordered nano channels and N species	Uniforming Zn plating; enhancing Zn^{2+} transport kinetics	2, 1 2, 2	1200 700	46
TiO_2&PVDF	Functional coating layer	Corrosion-inhibition and electrodeposition-redirection	Uniforming Zn plating; suppressing Zn corrosion	0.885, 0.885 8.85, 8.85	2000 250	49
IL skinny gel	Functional coating layer	Water-repellent	Suppressing side reactions	0.1, 0.1 0.5 1.8	1000 400	22
Nafion-Zn–X	Functional coating layer	Ion transport channel	Suppressing dendrite growth and side reactions	1, 0.5 1, 10	1000 >1000	50
ZnF_2	Solid electrolyte interphase	Zn^{2+} conducting; water-proof SEI	Suppressing Zn corrosion and dendrite growth	0.5 0.25	>3000	2
$Zn_3(PO_4)_2{\cdot}4H_2O$	Solid electrolyte interphase	Dense, stable, and Zn^{2+}-conductive	Suppressing side reactions	1, 1 1, 5	1200 800	13
$Zn_{12}(SO_4)_3Cl_3(OH)_{15}{\cdot}5H_2O$/$ZnSO_3$/ZnS	Solid electrolyte interphase	Dense and self-repaired interphase	Suppressing hydrogen evolution reaction	0.5, 0.5	1000	23
ZnF_2-$Zn_5(CO_3)_2(OH)_6$-organic	Solid electrolyte interphase	Electrically insulating but ionically conductive SEI	Promoting Zn^{2+} diffusion; suppressing hydrogen evolution reaction	0.5, 0.5	1200	25
ZnS	Solid electrolyte interphase	Regulable interphase	Suppressing Zn corrosion and dendrite growth	2.0, 2.0	1100	55
ZnSe	Solid electrolyte interphase	Low polarization voltage	Suppressing Zn corrosion; zincophobic	1.0, 1.0 10, 1.0	1500 1500	56
ZCO	Solid electrolyte interphase	Electrical insulation but ion conductive SEI	Promoting electric field distribution; inhibiting dendrite growth	1.0, 1.0 2.0, 2.0	1400 1400	57

see, the performances of SEI-protected AZIBs are far from the expectation. Therefore, selecting more suitable additives and applying more advanced *in situ*/*ex situ* techniques, including transmission electron microscopy (TEM), atomic force microscopy (AFM), secondary ion mass spectroscopy (SIMS), *etc*., are encouraged to provide more solid evidence to understand the microstructure, composition, thickness, and working mechanism of the *in situ* formed SEI films. In the meantime, some electrolyte additives can also suppress HER and dendrites without the formation of specific SEI films.[58,59] Those additives can regulate the Zn^{2+} solvation structure to break the H-bond network and eliminate water participation.[60] For that reason, the mechanism and function of selected electrolyte additives should be explained before performing the above characterizations. To better compare the relationship between properties and electrochemical performance of artificial Interphases, the interfacial materials, types, characteristics, major functions, testing conditions, and electrochemical performances of different materials relevant to artificial interphases are summarized in Table 1.

4. Conclusion and perspectives

Different from the mechanism of traditional batteries operated in organic electrolytes, in which the metallic anodes are protected by the self-produced SEI film, the AZIBs operated in aqueous electrolytes are suffering from severe hydrogen evolution reactions and metallic dendrites because of the absence of an efficient SEI film. Therefore, artificially regulating the Zn/electrolyte interphase has become increasingly important. Functional layer coating and *in situ* solid electrolyte interphase formation could be promising solutions to the undesired dendrites and parasitic reactions on the Zn anode. A growing body of research has revealed that using artificial interphase engineering to stabilize aqueous zinc metal anodes could realize the stable Zn plating/stripping under high power and high capacity. Despite the growing interest in artificial interphase engineering in recent years, there are many potential issues and perspectives to be discussed. For functional coating layers, there are a variety of potential materials in different functions, which imply more possibilities to solve the above issues of the Zn anode. Indeed, the coating layers with multi-functions that act as buffer interphase can avoid the direct contact of Zn metal within the aqueous electrolyte. However, the physical coating is hard to form an even interphase for Zn deposition. Tightly bonding the coating layer and Zn metal at the atomic level by the chemical bond is strongly recommended to bridge the gap between the protective layer and Zn anode. Besides, the external coating strategy with poor self-repairability and loose contacts to Zn anode will be a problem for the stability of long-term cycling. Therefore, more research interest should focus on improving reaction kinetics and interphase stability in electrolyte/coating layer/Zn anode, with respects to ionic conductivity, thickness, the energy barrier of Zn^{2+} transferring between the protective layer and Zn anode, which would fundamentally aid the development of functional coating layers. For solid electrolyte interphase, the strategy of *in situ* synthesis of assisted stable SEI films, which are tightly bonded to the Zn anode is a good choice for uniform Zn plating and self-repairable SEI growth in the long run. While the formation and growth processes of SEI involved in multiple chemical reactions are sophisticated and lacking in characterization. It would be necessary to do more fundamental works that focus on mechanisms, composition, formation, and function. On the basis of developing the practically viable AZIBs, we believe that the in-depth understanding of artificial interphases in mechanism and interphase stability is the key to shed light on its future development.

Conflicts of interest

There are no conflicts to declare.

Acknowledgements

The authors are grateful for financial support from the Fundamental Research Funds for the Central Universities (531118010111; 531118010633) and National Natural Science Foundation of China (52103313; 22109041).

References

1 Z. Yi, G. Chen, F. Hou, L. Wang and J. Liang, *Adv. Energy Mater.*, 2020, **11**, 2003065.
2 L. Cao, D. Li, T. Pollard, T. Deng, B. Zhang, C. Yang, L. Chen, J. Vatamanu, E. Hu, M. J. Hourwitz, L. Ma, M. Ding, Q. Li, S. Hou, K. Gaskell, J. T. Fourkas, X. Q. Yang, K. Xu, O. Borodin and C. Wang, *Nat. Nanotechnol.*, 2021, **16**, 902–910.
3 S. Chu and A. Majumdar, *Nature*, 2012, **488**, 294–303.
4 J. Ma, S. Zheng, P. Das, P. Lu, Y. Yu and Z.-S. Wu, *Small Struct.*, 2020, **1**, 2000053.
5 S. F. Ye, L. F. Wang, F. F. Liu, P. C. Shi and Y. Yu, *eScience*, 2021, DOI: 10.1016/j.esci.2021.09.003.
6 D. Wang, Y. Liu, G. Li, C. Qin, L. Huang and Y. Wu, *Adv. Funct. Mater.*, 2021, **31**, 2106740.
7 Z. Zhu, Y. Tang, W. Leow, H. Xia, Z. Lv, J. Wei, X. Ge, S. Cao, Y. Zhang, W. Zhang, H. Zhang, S. Xi, Y. Du and X. Chen, *Angew. Chem., Int. Ed.*, 2019, **58**, 3521–3526.
8 Z. Yan, Q. Tian, Y. Liang, L. Jing, Z. Hu, W. Hua, A. Tayal, W. Lai, W. Wang, J. Peng, Y.-X. Wang, J. Liu, S.-L. Chou, G.-Q. Lu, H. Liu and S.-X. Dou, *Cell Rep. Phys. Sci.*, 2021, **2**, 100539.
9 W. Lu, C. Zhang, H. Zhang and X. Li, *ACS Energy Lett.*, 2021, **6**, 2765–2785.
10 V. Verma, S. Kumar, W. Manalastas and M. Srinivasan, *ACS Energy Lett.*, 2021, **6**, 1773–1785.
11 H. Wang, R. Tan, Z. Yang, Y. Feng, X. Duan and J. Ma, *Adv. Energy Mater.*, 2020, **11**, 2000962.

12 D. Han, S. Wu, S. Zhang, Y. Deng, C. Cui, L. Zhang, Y. Long, H. Li, Y. Tao, Z. Weng, Q.-H. Yang and F. Kang, *Small*, 2020, **16**, 2001736.
13 X. Zeng, J. Mao, J. Hao, J. Liu, S. Liu, Z. Wang, Y. Wang, S. Zhang, T. Zheng, J. Liu, P. Rao and Z. Guo, *Adv. Mater.*, 2021, **33**, 2007416.
14 Q. Li, Y. Zhao, F. Mo, D. Wang, Q. Yang, Z. Huang, G. Liang, A. Chen and C. Zhi, *EcoMat*, 2020, **2**, e12035.
15 X. Wang and Z.-S. Wu, *EcoMat*, 2020, **2**, e12042.
16 Z. Miao, M. Du, H. Li, F. Zhang, H. Jiang, Y. Sang, Q. Li, H. Liu and S. Wang, *EcoMat*, 2021, **3**, e12125.
17 F. Mo, G. Liang, D. Wang, Z. Tang, H. Li and C. Zhi, *EcoMat*, 2019, **1**, e12008.
18 Q. Lu, C. Liu, Y. Du, X. Wang, L. Ding, A. Omar and D. Mikhailova, *ACS Appl. Mater. Interfaces*, 2021, **13**, 16869–16875.
19 Y. Chu, S. Zhang, S. Wu, Z. Hu, G. Cui and J. Luo, *Energy Environ. Sci.*, 2021, **14**, 3609–3620.
20 Z. Zhao, J. Zhao, Z. Hu, J. Li, J. Li, Y. Zhang, C. Wang and G. Cui, *Energy Environ. Sci.*, 2019, **12**, 1938–1949.
21 H. He and J. Liu, *J. Mater. Chem. A*, 2020, **8**, 22100–22110.
22 D. Lee, H.-I. Kim, W.-Y. Kim, S.-K. Cho, K. Baek, K. Jeong, D. B. Ahn, S. Park, S. J. Kang and S.-Y. Lee, *Adv. Funct. Mater.*, 2021, **31**, 2103850.
23 L. Cao, D. Li, E. Hu, J. Xu, T. Deng, L. Ma, Y. Wang, X.-Q. Yang and C. Wang, *J. Am. Chem. Soc.*, 2020, **142**, 21404–21409.
24 L. Cao, D. Li, F. A. Soto, V. Ponce, B. Zhang, L. Ma, T. Deng, J. M. Seminario, E. Hu, X.-Q. Yang, P. B. Balbuena and C. Wang, *Angew. Chem., Int. Ed.*, 2021, **60**, 18845–18851.
25 D. Li, L. Cao, T. Deng, S. Liu and C. Wang, *Angew. Chem., Int. Ed.*, 2021, **60**, 13035–13041.
26 H. Yan, S. Li, Y. Nan, S. Yang and B. Li, *Adv. Energy Mater.*, 2021, **11**, 2100186.
27 Z. Zhu, Y. Tang, Z. Lv, J. Wei, Y. Zhang, R. Wang, W. Zhang, H. Xia, M. Ge and X. Chen, *Angew. Chem., Int. Ed.*, 2018, **57**, 3656–3660.
28 X. Zhang, J. Li, D. Liu, M. Liu, T. Zhou, K. Qi, L. Shi, Y. Zhu and Y. Qian, *Energy Environ. Sci.*, 2021, **14**, 3120–3129.
29 G. Liang and C. Zhi, *Nat. Nanotechnol.*, 2021, **16**, 854–855.
30 Q. Jin, X. Zhang, H. Gao and Z. Zhang, *J. Mater. Chem. A*, 2020, **8**, 8979–8988.
31 P. Cao, X. Zhou, A. Wei, Q. Meng, H. Ye, W. Liu, J. Tang and J. Yang, *Adv. Funct. Mater.*, 2021, **31**, 2100398.
32 P. Liu, Z. Zhang, R. Hao, Y. Huang, W. Liu, Y. Tan, P. Li, J. Yan and K. Liu, *Chem. Eng. J.*, 2021, **403**, 126425.
33 Q. Zhang, J. Luan, Y. Tang, X. Ji and H. Wang, *Angew. Chem., Int. Ed.*, 2020, **59**, 13180–13191.
34 L. Ma, Q. Li, Y. Ying, F. Ma, S. Chen, Y. Li, H. Huang and C. Zhi, *Adv. Mater.*, 2021, **33**, 2007406.
35 L. Kang, M. Cui, F. Jiang, Y. Gao, H. Luo, J. Liu, W. Liang and C. Zhi, *Adv. Energy Mater.*, 2018, **8**, 1801090.
36 P. Liang, J. Yi, X. Liu, K. Wu, Z. Wang, J. Cui, Y. Liu, Y. Wang, Y. Xia and J. Zhang, *Adv. Funct. Mater.*, 2020, **30**, 1908528.
37 M. Liu, J. Cai, H. Ao, Z. Hou, Y. Zhu and Y. Qian, *Adv. Funct. Mater.*, 2020, **30**, 2004885.
38 Q. Zhang, J. Luan, X. Huang, Q. Wang, D. Sun, Y. Tang, X. Ji and H. Wang, *Nat. Commun.*, 2020, **11**, 3961.
39 C. Deng, X. Xie, J. Han, Y. Tang, J. Gao, C. Liu, X. Shi, J. Zhou and S. Liang, *Adv. Funct. Mater.*, 2020, **30**, 2000599.
40 H. Yan, S. Li, Y. Nan, S. Yang and B. Li, *Adv. Energy Mater.*, 2021, **11**, 2100186.
41 Y. Yang, C. Liu, Z. Lv, H. Yang, X. Cheng, S. Zhang, M. Ye, Y. Zhang, L. Chen, J. Zhao and C. C. Li, *Energy Storage Mater.*, 2021, **41**, 230–239.
42 Q. Yang, Y. Guo, B. Yan, C. Wang, Z. Liu, Z. Huang, Y. Wang, Y. Li, H. Li, L. Song, J. Fan and C. Zhi, *Adv. Mater.*, 2020, **32**, 2001755.
43 J. Ding, Y. Liu, S. Huang, X. Wang, J. Yang, L. Wang, M. Xue, X. Zhang and J. Chen, *ACS Appl. Mater. Interfaces*, 2021, **13**, 29746–29754.
44 M. Zhu, J. Hu, Q. Lu, H. Dong, D. D. Karnaushenko, C. Becker, D. Karnaushenko, Y. Li, H. Tang, Z. Qu, J. Ge and O. G. Schmidt, *Adv. Mater.*, 2021, **33**, 2007497.
45 X. Pu, B. Jiang, X. Wang, W. Liu, L. Dong, F. Kang and C. Xu, *Nano-Micro Lett.*, 2020, **12**, 152.
46 X. Liu, F. Yang, W. Xu, Y. Zeng, J. He and X. Lu, *Adv. Sci.*, 2020, **7**, 2002173.
47 R. Yuksel, O. Buyukcakir, W. K. Seong and R. S. Ruoff, *Adv. Energy Mater.*, 2020, **10**, 1904215.
48 Z. Wang, J. Huang, Z. Guo, X. Dong, Y. Liu, Y. Wang and Y. Xia, *Joule*, 2019, **3**, 1289–1300.
49 R. Zhao, Y. Yang, G. Liu, R. Zhu, J. Huang, Z. Chen, Z. Gao, X. Chen and L. Qie, *Adv. Funct. Mater.*, 2021, **31**, 2001867.
50 Y. Cui, Q. Zhao, X. Wu, X. Chen, J. Yang, Y. Wang, R. Qin, S. Ding, Y. Song, J. Wu, K. Yang, Z. Wang, Z. Mei, Z. Song, H. Wu, Z. Jiang, G. Qian, L. Yang and F. Pan, *Angew. Chem., Int. Ed.*, 2020, **59**, 16594–16601.
51 H. He, H. Qin, J. Wu, X. Chen, R. Huang, F. Shen, Z. Wu, G. Chen, S. Yin and J. Liu, *Energy Storage Mater.*, 2021, **43**, 317–336.
52 F. Tao, Y. Liu, X. Ren, J. Wang, Y. Zhou, Y. Miao, F. Ren, S. Wei and J. Ma, *J. Energy Chem.*, 2022, **66**, 397–412.
53 G. Liang, F. Mo, Q. Yang, Z. Huang, X. Li, D. Wang, Z. Liu, H. Li, Q. Zhang and C. Zhi, *Adv. Mater.*, 2019, **31**, 1905873.
54 J. Shin, J. Lee, Y. Park and J. W. Choi, *Chem. Sci.*, 2020, **11**, 2028–2044.
55 J. Hao, B. Li, X. Li, X. Zeng, S. Zhang, F. Yang, S. Liu, D. Li, C. Wu and Z. Guo, *Adv. Mater.*, 2020, **32**, 2003021.
56 L. Zhang, B. Zhang, T. Zhang, T. Li, T. Shi, W. Li, T. Shen, X. Huang, J. Xu, X. Zhang, Z. Wang and Y. Hou, *Adv. Funct. Mater.*, 2021, **31**, 2100186.
57 X. Xu, Y. Chen, D. Zheng, P. Ruan, Y. Cai, X. Dai, X. Niu, C. Pei, W. Shi, W. Liu, F. Wu, Z. Pan, H. Li and X. Cao, *Small*, 2021, **17**, 2101901.
58 Z. Hou, Z. Lu, Q. Chen and B. Zhang, *Energy Storage Mater.*, 2021, **42**, 517–525.
59 A. Naveed, H. Yang, J. Yang, Y. Nuli and J. Wang, *Angew. Chem., Int. Ed.*, 2019, **58**, 2760–2764.
60 Q. Zhang, Y. Ma, Y. Lu, X. Zhou, L. Lin, Z. Yan, Q. Zhao, K. Zhang and J. Chen, *Angew. Chem., Int. Ed.*, 2021, **60**, 23357–23364.

61 W. Xin, L. Miao, L. Zhang, H. Peng, Z. Yan and Z. Zhu, *ACS Mater. Lett.*, 2021, **3**, 1819–1825.
62 L. Zhang, L. Miao, W. Xin, H. Peng, Z. Yan and Z. Zhu, *Energy Storage Mater.*, 2022, **44**, 408–415.
63 P. Li, H. Kim, J. Ming, H.-G. Jung, I. Belharouak and Y.-K. Sun, *eScience*, 2021, DOI: 10.1016/j.esci.2021.10.002.
64 S. Ye, L. Wang, F. Liu, P. Shi and Y. Yu, *eScience*, 2021, DOI: 10.1016/j.esci.2021.09.003.